

Article

The Arrangement of the Osteons and Kepler's Conjecture

Marco Zedda 

Department of Veterinary Medicine, University of Sassari, 07100 Sassari, Italy; mzedda@uniss.it

Abstract: The studies of bone tissue have mainly highlighted the morphometrical characteristics of the osteons, rather than their spatial distribution. This work aimed to verify if the topographical distribution of the osteons responds to geometrical order. From an analysis of hundreds of bone sections of domestic and wild mammals collected over 60 years, it is evident that the spatial distribution of osteons varies from a random arrangement in the irregular Haversian tissue to an ordered geometric arrangement in the dense Haversian tissue. In this work, a new method of classification of Haversian bone tissue was introduced based on the number of points of contact that the perimeter of an osteon has with neighboring osteons. When the functional commitment of the bone is maximum to resist biomechanical stresses, the osteons are smaller and crammed adjacent to each other as if to occupy less space. Their spatial arrangement, in this case, reminds us of Kepler's conjecture, which predicts the ideal arrangement that spheres must have to occupy as little space as possible. The conjecture was elaborated by Kepler in the Seventeenth Century to solve the practical problem linked to the need to transport the largest number of cannonballs in warships.

Keywords: bone tissue; osteon; Haversian tissue; interosteonal area; Kepler's conjecture

1. Introduction

The study of the bone microstructure never ceases to surprise researchers with how much data and observations can be extracted. Unlike what can be considered by ordinary people, i.e., that bone tissue has a rigid and immobile structure over time, in the last two centuries, there has been an increase in evidence that bones are plastic structures that adapt to the biomechanical needs of individuals through modifications of their microstructure. In addition to the genetic predisposition related to the taxonomic position of species and breeds, numerous factors interfere in modifying the bone microstructure, such as age, sex, body mass, lifestyle, pathological conditions, and dietary pattern [1–5]. Another factor among the most-important is the exposure to mechanical stress due to locomotion, which influences the bone microstructure throughout different movements and gaits [6,7]. Since locomotion modalities vary greatly in the animal kingdom, on the bones of the skeleton and in the course of life, the possibilities of bone microstructural modifications are very wide. Bone tissue shows a complex arrangement of structures at different length scales, which perform mechanical, biological, and chemical functions such as providing structural support, protection of internal organs and tissues, and mineral storage [8,9]. From a histological point of view, not only has each taxonomical category of vertebrates a general pattern recognizable in the skeleton [10], but it is also shown for each bone of the same skeleton histomorphometrical features that are strictly related to the biomechanical loads to which they are exposed [4].

In adult bone tissue of the most-evolved vertebrates, the structural component that has attracted interest from researchers and explains many of the bone properties is undoubtedly the secondary osteon, also known as the Haversian system. Each osteon consists of concentric layers, or bone lamellae, surrounding a central canal, named the Haversian canal, flown by blood vessels and nerves. The compact bone tissue containing osteons is classified as Haversian tissue, which shows two types characterized by the different closeness of the osteons. In particular, the irregular Haversian tissue has few osteons widely separated by



Citation: Zedda, M. The Arrangement of the Osteons and Kepler's Conjecture. *Appl. Sci.* **2023**, *13*, 5170. <https://doi.org/10.3390/app13085170>

Academic Editor: Miguel Ángel Maté-González

Received: 24 March 2023

Revised: 4 April 2023

Accepted: 19 April 2023

Published: 21 April 2023



Copyright: © 2023 by the author. Licensee MDPI, Basel, Switzerland. This article is an open access article distributed under the terms and conditions of the Creative Commons Attribution (CC BY) license (<https://creativecommons.org/licenses/by/4.0/>).

abundant interstitial bone, whereas numerous osteons form the dense Haversian tissue, close together and connected by more or less scarce interstitial bone [11,12]. The closeness of the osteons employed to distinguish these two types of Haversian tissue appears not always unequivocally applied by researchers, the closeness a being a somewhat subjective concept. Contributing to the identification of different osteon distribution patterns in the dense Haversian tissue was one of the aims of this study.

As regards the osteons, the descriptive studies of bone tissue in different animal species have mainly highlighted their morphological and morphometric characteristics rather than their spatial distribution. In long bone transversal sections, the Haversian systems, which are secondary osteons and, henceforth, in this text named osteons, appear circular or elliptical in shape since their three-dimensional cylindrical structure extends along the major axis of the bones. Histomorphometrical research has been carried out to evaluate the number of bone lamellae, the size of the osteons, and their Haversian canals by means of measurements of the maximum diameter, minimum diameter, perimeter, area, and relative ratios. These parameters were taken into account, among others, with trying to identify the animal species [13–16], especially to distinguish human skeletal remains from animals [3,17–21], or to study the age of death on the base of the skeletochronology [7,22], or to distinguish domestic from wild mammals [23,24]. Assuming the idea that the bone area subjected to compression loads shows a higher amount of osteons [25,26], the frequency and distribution of the osteons have also attracted interest in order to analyze biomechanical features [27–32] or to reconstruct the lifestyle of extinct vertebrates [33–35]. The frequency of osteons in a bone section, indicated by the osteon population density, has been described by calculating the number of osteons in 1 mm². This value is very useful to appreciate the scarcity or richness of osteons in an area. However, it gives us little information on the mutual relationship among the osteons, for example whether the osteons are in contact with each other or not, since it depends on their size.

This work aimed to verify if the arrangement of the osteons in the dense Haversian tissue could be evaluated as random or, on the contrary, in some cases, if it responds to a precise strategy that improves bone performance to resist biomechanical stresses better. In particular, attention will be paid to observing how the osteons are arranged when their number increases following greater mechanical stress.

2. Materials and Methods

For this study, hundreds of histological slides of bone sections collected during the last 60 years in the laboratory of the Anatomy of the Department of Veterinary Medicine at the University of Sassari (Italy) were checked. This collection was created from bones of healthy individuals, regularly slaughtered or who died of natural causes at the veterinary clinic of the Department and belonging to domestic animals, such as horses (*Equus caballus*), cows (*Bos taurus*), pigs (*Sus scrofa domestica*), sheep (*Ovis aries*), goats (*Capra hircus*), and dogs (*Canis familiaris*), and wild animals such as deer (*Cervus elaphus*), wild boars (*Sus scrofa*), mouflons (*Ovis musimon*), and foxes (*Vulpes vulpes*). All these slides were realized in the past few decades by the wear method and now briefly reported. Long bones were crosscut at the level of the smallest breadth of their diaphyses using an electrical saw to obtain 2 mm-thick sections. The air-dried bony rings were ground and thinned using a fine sandpapering machine. Then, the samples were sanded by hand with emery paper to obtain about 50 µm-thick sections. After thorough washing to remove the debris, the cross-sections were fixed onto glass slides with Eukitt (Merck, Darmstadt, Germany). Histological slides were observed and photographed using a Zeiss Axiophot microscope at 2.5×, 10×, and 20× magnifications (Zeiss, Jena, Germany). Sections were scanned with a digital scanner (Motic Easy Scan One, Motic, Hong Kong) using a PlanApochromat 10×/0.3 objective (Zeiss, Jena, Germany) to appreciate the osteon arrangement better. All slides were deposited at the Department of Veterinary Medicine of the University of Sassari. In order to evaluate the relation between the number of osteons and their arrangement, some measurements were taken or calculated, according to the report [36] of the Histomorphometry Nomenclature

Committee of the American Society for Bone and Mineral Research (ASBMR). More in detail, the measurements were mean value between the minimum and maximum diameters of the osteons (On.Dm) and the area of osteons (On.Ar) taken by means of the software Scion Image 3.2 (Scion Corporation, Frederick, MD, USA). The osteon population density (On.Dn), which describes the number of osteons per square millimeter, was also assessed, considering only the intact osteons. The interosteonal area was calculated as the difference between the area of the section and the total area occupied by intact osteons.

3. Results

Osteons with typical morphological features characterized by concentric bone lamellae surrounding a Haversian canal were present in all the species examined. They showed high variability in size, including the number of bone lamellae, the diameter of the osteons, and consequently, the perimeter and the area of the osteons. This variability depended on the species and the bone considered and often was present in the same histological slide. The main morphological and morphometrical features of the osteons in the species observed are reported in Table 1, where in extreme synthesis, it can be noted that the horse osteons were more extensive than those of ruminants (cows, goats, sheep, mouflons, deer), themselves larger than those of suids (domestic pigs, wild boars), themselves larger than those of carnivores (dogs, foxes).

Table 1. Histomorphometrical data of the Haversian bone tissue in different species ¹.

	Osteon Measurements			Haversian Bone Tissue		
	n	On.Dm	On.Ar	On.Dn	Irregular	Dense
Horse (<i>Equus caballus</i>)	147	198.4 ± 32.9	31,582.5 ± 4386.2	5.1	+	++++
Cow (<i>Bos taurus</i>)	134	164.7 ± 27.3	19,538.0 ± 2708.5	4.4	++	+++
Deer (<i>Cervus elaphus</i>)	43	135.9 ± 18.1	13,613.3 ± 2144.6	4.8	++	+++
Pig (<i>Sus scrofa domestica</i>)	103	138.6 ± 41.6	14,721.4 ± 1928.4	2.9	+++	++
Wild boar (<i>Sus scrofa</i>)	98	179.3 ± 25.8	22,167.1 ± 3319.7	3.9	++	+++
Sheep (<i>Ovis aries</i>)	170	128.2 ± 33.2	15,182.4 ± 2361.5	3.2	++++	+
Goat (<i>Capra hircus</i>)	162	124.7 ± 24.5	14,601.3 ± 2173.8	3.8	+++	+
Mouflon (<i>Ovis musimon</i>)	109	156.6 ± 26.4	18,039.2 ± 2549.3	4.1	+++	++
Fox (<i>Vulpes vulpes</i>)	56	139.4 ± 37.0	15,496.7 ± 1838.2	2.9	+++	++
Dog (<i>Canis familiaris</i>)	74	125.2 ± 22.8	14,083.2 ± 2071.6	2.4	++++	+

¹ The osteon diameter (On.Dm) and osteon area (On.Ar) are the mean values of one hundred measurements (expressed, respectively, in μ and μ^2); n, number of osteons measured; \pm standard deviation. Qualitative observations express the frequency of the irregular Haversian and dense Haversian tissues. From + to ++++ are indicated the growing amount of two types of Haversian bone tissue.

Regarding the type of bone tissue, besides plexiform tissue, both irregular Haversian and dense Haversian tissue were present in all species with different extensions (Figure 1). In ascending order of greatest presence of dense Haversian tissue than irregular Haversian tissue can be listed carnivores, suids, ruminants, and horses. Moreover, dense Haversian tissue is generally larger in the wild species (deer, mouflons, wild boars, foxes) than in domestic animals.

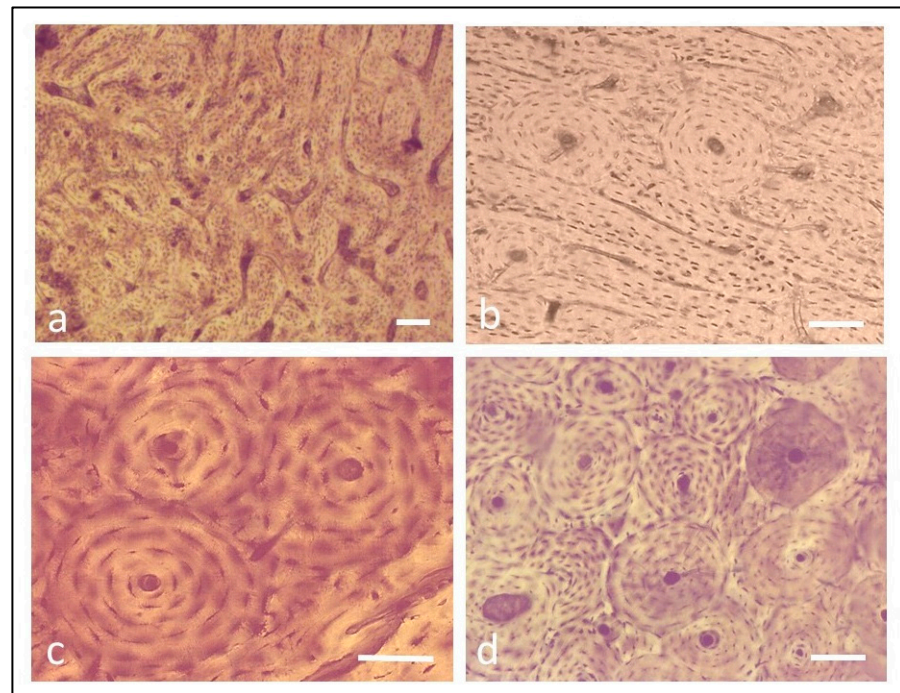


Figure 1. The main types of bone tissue present in mammals. (a) Plexiform tissue (*Sus scrofa*); (b) irregular Haversian tissue with few osteons isolated and far from each other (*Ovis aries*); (c) dense Haversian tissue with an islet of three osteons (*Bos taurus*); (d) dense Haversian tissue with many osteons crammed (*Equus caballus*). Bar = 40 μm .

The main aim of this work was to observe different arrangements of the osteons. It varied from a case of random dispersion, where the osteons were few and far from each other, to a condition where the osteons were numerous and cramped. The scenario of the osteon arrangement is often complex because osteons with different sizes can be present in the same field, which aggravates the possibility of easily recognizing the schemes of the osteon layout. The arrangement typical of the irregular Haversian tissue could be better defined as the tissue where the osteons are not in contact with each other and then their cement line, that is the periphery of each osteon, does not even have a single point in common with the others (Figure 1b). Therefore, in this tissue type, the interosteonal area is very wide.

3.1. Proposal of Identification of Subtypes of the Dense Haversian Tissue

In the dense Haversian tissue, the osteons appear close and in contact with each other, regardless of their size. They showed one or more points in common at the level of their cement line, and the number of points in common could be helpful in order to recognize different subtypes of this tissue and better evaluate the osteon arrangement. Indeed, these values range from: (1) when two osteons are in contact, but distant from others; (2) when each osteon is in contact with two other osteons and then forms an isolated group of three osteons (Figure 1c), and so on, until they achieve there eight or more contacts (Figure 1d). Based on this point of view, three subtypes of dense Haversian tissue (H_1 , H_2 , H_3) are here proposed. The H_1 dense Haversian tissue is characterized by osteons with different sizes and in contact with each other with a variable number of points in common starting from one. Its interosteonal area is very irregular in shape as limited by the cement line of the neighboring osteons. It is the subtype of dense Haversian tissue most-frequent and detectable in all the species examined. The H_2 dense Haversian tissue contains osteons of almost the same size arranged side by side to form overlapping lines so that each osteon has four points in common with the neighboring osteons (Figure 2a,b). In this case, the interosteonal area comprises four osteons, and it is quadrangular in shape

with concave sides. This subtype is not frequent and can be observed in ruminants and suids during the first phases of remodelling when the plexiform bone tissue typical of juvenile individuals change into irregular Haversian tissue and secondary osteons appear. The H₃ dense Haversian tissue is formed by osteons of the same size arranged side by side to form overlapping lines so that each osteon is in contact with six others (Figure 2c,d). Its interosteonal area is comprised between only three osteons, and it is triangular in shape with concave sides. This subtype of dense Haversian tissue is present overall, where the bones are subjected to heavy biomechanical stress, such as in some areas exposed to compression loads of long equine bones.

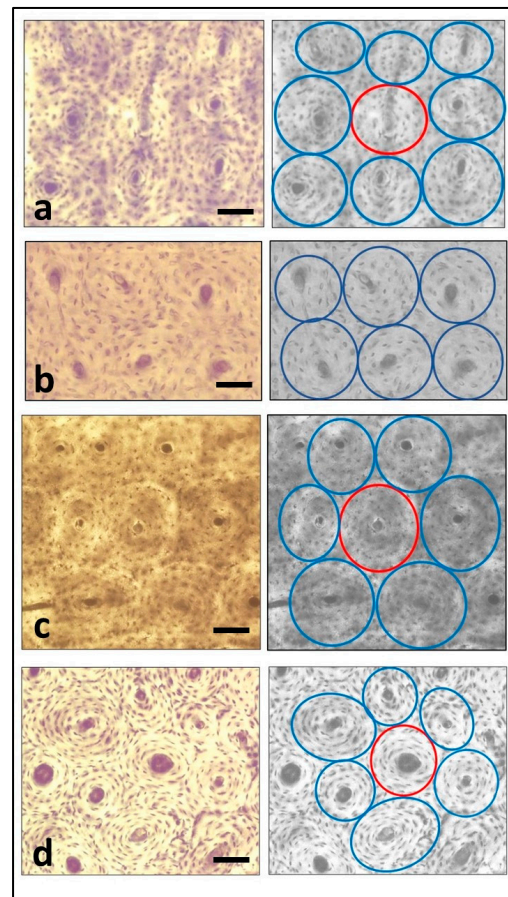


Figure 2. Dense Haversian tissue. **(Left)** Original microphotos; **(Right)** osteons are highlighted with circles to evaluate the common points with neighboring osteons. **(a,b)** H₂ subtype, where each osteon is in contact with 4 other osteons ((a) *Capra hircus*; (b) *Sus scrofa*). **(c,d)** H₃ subtype, where each osteon is in contact with 6 other osteons ((c) *Ovis musimon*; (d) *Equus caballus*). The circles correspond to osteons. In H₃ subtype an osteon (red circle) is surrounded by 6 osteons (blue circles). Bar = 40 μ m.

3.2. The Interosteonal Area and Its Theoretical Calculation

As mentioned before, all the surface not occupied by secondary osteons is considered an interosteonal area. While the H₁ interosteonal area is very extensive and widely communicating to surround isolated osteons and more or less numerous groups of osteons, in the H₂ and H₃ subtypes, the interosteonal area is limited and forms small islets surrounded by osteons. More precisely, the shape of these islets is quadrangular with concave sides in H₂ and triangular with concave sides in H₃. In the H₁ subtype, the interosteonal area can be easily calculated as the difference between the area considered and the sum of osteonal areas. In contrast, in H₂ and H₃ subtypes, the interosteonal area could be mathematically calculated besides the method for the H₁ subtype. In detail, in the H₂ subtype, the interosteonal area can be considered the difference between the square drawn on the central point

of the Haversian canal of four adjacent osteons and the area of one osteon (corresponding to four cloves of a quarter of osteon) (Figure 3a). With r indicating the radius of the osteon, the quadrangular interosteonal area can be easily calculated with this mathematical procedure:

$$(2r)^2 - \pi r^2 = 4r^2 - \pi r^2 = (4 - \pi)r^2$$

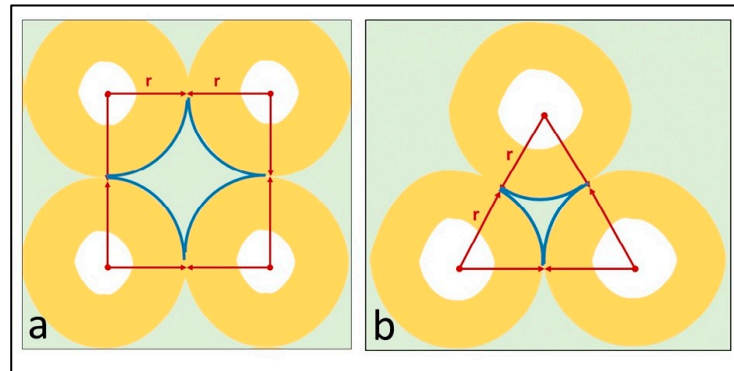


Figure 3. Schematic representations of the interosteonal area surrounded by the neighboring osteons in the H₂ subtype (a) and H₃ subtype (b) of dense Haversian tissue for its theoretical calculation.

In the H₃ subtype, the interosteonal area can be considered as the difference between the equilateral triangle drawn on the central point of the Haversian canal of three adjacent osteons and the area occupied by three cloves of a sixth of an osteon (Figure 3b). Firstly, the formula to determine the area of an equilateral triangle knowing Side l (that is $2r$) can be applied:

$$l^2 \frac{\sqrt{3}}{4} = (2r)^2 \frac{\sqrt{3}}{4} = r^2 \sqrt{3}$$

The area occupied by three cloves of a sixth osteon is

$$3 \frac{1}{6} \pi r^2 = \frac{1}{2} \pi r^2$$

Thus, the interosteonal area in the H₃ subtype is

$$r^2 \sqrt{3} - \frac{1}{2} \pi r^2 = (\sqrt{3} - \frac{1}{2} \pi) r^2$$

It can be noted that the interosteonal area of the H₃ subtype is smaller than that of the H₂ subtype, since:

$$\sqrt{3} - \frac{1}{2} \pi < 4 - \pi$$

3.3. Comparison between the Theoretical and Real Calculation of the Interosteonal Area

The formulae described above for the H₂ and H₃ subtypes led to a theoretical calculation that would be valid under the conditions of perfect equality and circularity of the osteons. The real calculation based on the difference of the total measured area occupied by intact osteons from the area of the section was similar to what was theoretically calculated. Indeed, the real extension of the interosteonal areas was about 8% higher than the theoretical values. The reason for this difference could be due to the fact that the osteons were not perfectly circular, but slightly elliptical. Rather than calculating the absolute value of the interosteonal area, it is much more useful to evaluate its relative value and the ratio between the interosteonal area and the total area considered. In the H₂ subtype, a square drawn so that the vertices correspond to the center of the Haversian canal of four adjacent osteons can be considered a repetitive modulus formed by four cloves of the quarter of the osteon delimiting the quadrangular interosteonal area. In this case, the percentual ratio expressed between the interosteonal and the area of the modulus was about 21.5%. In the H₃ subtype, the repetitive modulus was triangular, and it was formed by three cloves of the sixth osteon delimiting the triangular interosteonal area. In this case, the percentual

ratio expressed between the interosteonal and the area of the modulus was about 9.4%. This means that the osteon arrangement in the H₃ subtype was the condition of minimum interosteonal area extension and maximum packing of the osteons (Figure 4).

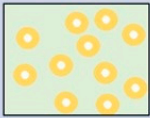
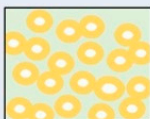


	Classification	Osteon arrangement	Number of osteons in contact	Interosteonal area	Ratio interosteonal area/total area
	irregular Haversian tissue	random dispersion of isolated osteons with different size. No points in common are present	0	irregular and abundant	50-90%
	dense Haversian tissue H1 subtype	osteons with different size in contact to form islets formed by a variable number of osteons completely surrounded by interosteonal area	variable	irregular and abundant	50-90%
	dense Haversian tissue H2 subtype	osteons with the same size arranged side by side to form overlapping lines so that each osteon has 4 points in common with the neighboring osteons	4	quadrangular shape with concave sides $(4 - \pi)r^2$	21.5%
	dense Haversian tissue H3 subtype	osteons with the same size, arranged side by side to form overlapping lines so that each osteon has 6 points in common with the neighboring osteons	6	triangular shape with concave sides $(\sqrt{3} - \frac{1}{2}\pi)r^2$	9.4%

Figure 4. Schematic differences among the subtypes of the Haversian tissue proposed.

4. Discussion

The results presented in this work highlighted the complexity of the Haversian tissue providing reading keys to describe the arrangement of the osteons. The presence of the osteons in the species analyzed confirmed general rules valid in mammals, such as their greater presence in animals most-engaged in biomechanical stress due to a high body mass and aptitude to high speeds and wild animals that generally have more intense locomotor activity than domestic animals. As regards the size of the osteons, among the factors that mainly influence it, the biomechanical stress to which the bones are subjected is the main one [28,29], whilst the body mass does not seem to matter much [37].

As is known, osteons can be considered as tridimensional structures organized to better resist mechanical stresses. Indeed, the central canal surrounded by some layers of bone lamellae gives to the osteon excellent properties to oppose the compression, torsion, and tension forces [38–40]. Osteons with different sizes can be present both in the irregular Haversian tissue and in the H₁ subtype of dense Haversian tissue. In these cases, the points of contact of the cement line with neighboring osteons can be variable in number depending on the closeness of the osteons. In the H₂ and H₃ subtypes, the sizes of the osteons are very similar and the osteonal arrangement is more regular with a geometrical character. As described before, the interosteonal area shrinks from the irregular Haversian tissue to the H₁ subtype of dense Haversian tissue, and so on, to the H₂ subtype and up to the H₃ subtype. This means that, according to the same order, the presence of osteons grows up, and then, the resistance to biomechanical stress increases in the same order (Figure 5). It should come as no surprise that these last two subtypes and, especially, H₃ are found in long bones highly exposed to stress.

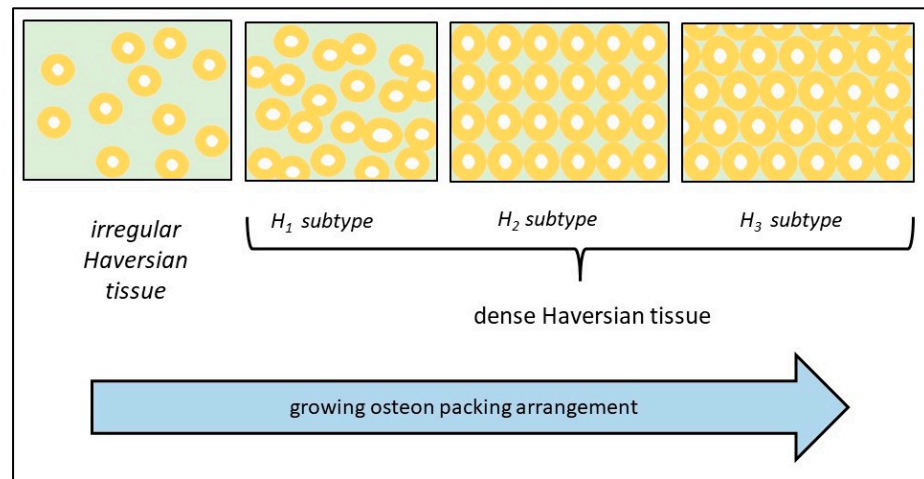


Figure 5. Schematic representation of the different osteon arrangements in Haversian bone tissue.

In the case of the H_3 subtype, it is as if the osteons were trying to arrange themselves in the best way to occupy less space. This consideration brings to mind Kepler's conjecture. It is a mathematical theorem about sphere arrangement in a limited space. The problem arose in the 16th Century when war ships carried cannonballs and needed to transport the largest amount of them in defined spaces. The solution of the problem was sought by mathematicians, astronomers, and other intellectuals of the time until Johannes Kepler (1571–1630) enunciated his conjecture. In 1611, Kepler wrote a short work, *Strena Seu de Nive Sexangula*, where he described for the first time the hexagonal symmetry of snowflakes, extending the discussion on the most-efficient arrangement for packing spheres [41]. Kepler's conjecture, for which, being a conjecture, it has not been possible to demonstrate the falsity and which is, therefore, presumed to be true, states that no arrangement of equally sized spheres filling a space has a greater average density than that of the hexagonal close packing arrangements [42–44]. The conjecture was enunciated thinking of cannonballs arranged in a space, but finds its analogy in the arrangement of the osteons in the H_3 subtype considering the spheres sectioned by a plane. Just as Kepler's conjecture predicts the maximum packing of the spheres when one sphere is in contact with six other spheres in the same plane, similarly in dense Haversian tissue, the maximum degree of packing occurs when the osteons are arranged in such a way that each is in contact with six other osteons, i.e., in the H_3 subtype of the dense Haversian tissue here described.

5. Conclusions

From observing hundreds of sections of bone tissue, some characteristic dispositions of the osteons were highlighted: from a sparse disposition in the irregular Haversian tissue to a regular one in which different degrees of packing can be distinguished, including in the more regular ones. This is the case where each osteon is in contact with 4 neighboring osteons and where each osteon is in contact with 6 neighboring osteons. This last arrangement is the one suggested in Kepler's conjecture and corresponds to the maximum degree of packing arrangement. The classification of the dense Haversian tissue here proposed can pave the way for a vast series of investigations from a biomechanical, anthropological, archaeozoological, and paleontological point of view, for example to help reconstruct the locomotor abilities of extinct animals.

Funding: This research received no external funding.

Institutional Review Board Statement: Not applicable.

Informed Consent Statement: Not applicable. This study did not require official or institutional ethical approval. The bone samples were taken from bones belonging to animals regularly butchered in local slaughterhouses or deaths from road accidents.

Data Availability Statement: All data are included in the Section 3 of the article.

Conflicts of Interest: The author declares no conflict of interest.

References

1. Frost, H.M. Secondary osteon population densities: An algorithm for estimating the missing osteons. *Yearb. Phys. Anthropol.* **1987**, *30*, 239–254. [[CrossRef](#)]
2. Ruffing, J.A.; Cosman, F.; Zion, M.; Tendy, S.; Garrett, P.; Lindsay, R.; Nieves, J.W. Determinants of bone mass and bone size in a large cohort of physically active young adult men. *Nutr. Metab.* **2006**, *3*, 14. [[CrossRef](#)] [[PubMed](#)]
3. Brits, D.; Steyn, M.; L'Abbé, E.N. A histomorphological analysis of human and non-human femora. *Int. J. Leg. Med.* **2014**, *128*, 369–377. [[CrossRef](#)] [[PubMed](#)]
4. Skedros, J.G.; Knight, A.N.; Clark, G.C.; Crowder, C.M.; Dominguez, V.M.; Qiu, S.; Mulhern, D.M.; Donahue, S.W.; Busse, B.; Hulsey, B.I.; et al. Scaling of Haversian canal surface area to secondary osteon bone volume in ribs and limb bones. *Am. J. Phys. Anthropol.* **2013**, *151*, 230–244. [[CrossRef](#)]
5. Felder, A.A.; Phillips, C.; Cornish, H.; Cooke, M.; Hutchinson, J.R.; Doube, M. Secondary osteons scale allometrically in mammalian humerus and femur. *R. Soc. Open Sci.* **2017**, *4*, 170431. [[CrossRef](#)]
6. Biewener, A.A. Biomechanical consequences of scaling. *J. Exp. Biol.* **2005**, *208*, 1665–1676. [[CrossRef](#)]
7. Babosová, R.; Zedda, M.; Belica, A.; Golej, M.; Chovancová, G.; Kalaš, M.; Vondráková, M. The enrichment of knowledge about the microstructure of brown bear compact bone tissue. *Eur. Zool. J.* **2022**, *89*, 615–624. [[CrossRef](#)]
8. Skerry, T.M. The response of bone to mechanical loading and disuse: Fundamental principles and influences on osteoblast/osteocyte homeostasis. *Arch. Biochem. Biophys.* **2008**, *473*, 117–123. [[CrossRef](#)]
9. Sabet, F.A.; Raeisi Najafi, A.; Hamed, E.; Jasiuk, I. Modelling of bone fracture and strength at different length scales: A review. *Interface Focus* **2016**, *6*, 20150055. [[CrossRef](#)]
10. Enlow, D.H.; Brown, S.O. A comparative histological study of fossil and recent bone tissues Part III. *Tex. J. Sci.* **1958**, *10*, 187–230.
11. Enlow, D.H.; Brown, S.O. A comparative Histological Study of fossil and Recent Bone Tissues. Part I. *Tex. J. Sci.* **1956**, *8*, 405–443.
12. Francillon-Vieillot, H.; de Bufrénil, V.; Castanet, J.; Geraudie, J.; Meunier, F.J.; Sire, J.Y.; Zylberberg, L.; de Ricqlès, A. Skeletal Biomineralization: Patterns, Processes and Evolutionary Trends. In *Microstructure and Mineralization of Skeletal Vertebral Tissues*; Carter, J.G., Ed.; Springer: Berlin, Germany, 1989; pp. 471–530.
13. Morales, J.P.; Ignacio, R.H.; Daniela, Z.; Ivan, S.H. Determination of the species from skeletal remains through histomorphometric evaluation and discriminant analysis. *Int. J. Morphol.* **2012**, *30*, 1035–1041. [[CrossRef](#)]
14. Zedda, M.; Lepore, G.; Manca, P.; Chisu, V.; Farina, V. Comparative bone histology of adult horses (*Equus caballus*) and cows (*Bos taurus*). *Anat. Histol. Embryol.* **2008**, *37*, 442–445. [[CrossRef](#)] [[PubMed](#)]
15. Zedda, M.; Palombo, M.R.; Brits, D.; Carcupino, M.; Sathe, V.; Cacchioli, A.; Farina, V. Differences in femoral morphology between sheep (*Ovis aries*) and goat (*Capra hircus*): Macroscopic and microscopic observations. *Zoomorphology* **2017**, *136*, 145–158. [[CrossRef](#)]
16. Gudea, A.I.; Stefan, A.C. Histomorphometric, fractal and lacunarity comparative analysis of sheep (*Ovis aries*), goat (*Capra hircus*) and roe deer (*Capreolus capreolus*) compact bone samples. *Folia Morphol.* **2013**, *72*, 239–248. [[CrossRef](#)]
17. Jowsey, J. Studies of Haversian systems in man and some animals. *J. Anat.* **1966**, *100*, 857–864.
18. Cuijpers, A.G.F.M. Histological identification of bone fragments in archaeology: Telling humans apart from horses and cattle. *Int. J. Osteoarchaeol.* **2006**, *16*, 165–180. [[CrossRef](#)]
19. Hillier, M.L.; Bell, L.S. Differentiating human bone from animal bone: A review of histological methods. *J. Forensic Sci.* **2007**, *52*, 249–263. [[CrossRef](#)]
20. Crescimanno, A.; Stout, S.D. Differentiating fragmented human and nonhuman long bone using osteon circularity. *J. Forensic Sci.* **2012**, *57*, 287–294. [[CrossRef](#)]
21. Dominguez, V.M.; Crowder, C.M. The utility of osteon shape and circularity for differentiating human and non-human haversian bone. *Am. J. Phys. Anthropol.* **2012**, *149*, 84–91. [[CrossRef](#)]
22. Nacarino-Meneses, C.; Jordana, X.; Köhler, M. First approach to bone histology and skeletochronology of *Equus hemionus*. *C. R. Palevol.* **2016**, *15*, 277–287. [[CrossRef](#)]
23. Giua, S.; Farina, V.; Cacchioli, A.; Ravanetti, F.; Carcupino, M.; Mohadero Novas, M.; Zedda, M. Comparative histology of the femur between mouflon (*Ovis aries musimon*) and sheep (*Ovis aries aries*). *J. Biol. Res.* **2014**, *87*, 74–77. [[CrossRef](#)]
24. Zedda, M.; Brits, D.; Giua, S.; Farina, V. Distinguishing domestic pig femora and tibiae from wild boar through microscopic analyses. *Zoomorphology* **2019**, *138*, 159–170. [[CrossRef](#)]
25. Mason, M.W.; Skedros, J.G.; Bloebaum, R.D. Evidence of strain-mode-related cortical adaptation in the diaphysis of the horse radius. *Bone* **1995**, *17*, 229–237. [[CrossRef](#)] [[PubMed](#)]
26. Matsuo, H.; Tsurumoto, T.; Maeda, J.; Saiki, K.; Okamoto, K.; Ogami-Takamura, K.; Kondo, H.; Tomita, M.; Yonekura, A.; Osaki, M. Investigating interindividual variations in cortical bone quality: Analysis of the morphotypes of secondary osteons and their population densities in the human femoral diaphysis. *Anat. Sci. Int.* **2019**, *94*, 75–85. [[CrossRef](#)]
27. Bigley, R.F.; Griffin, L.V.; Christensen, L.; Vandenbosch, R. Osteon interfacial strength and histomorphometry of equine cortical bone. *J. Biomech.* **2006**, *39*, 1629–1640. [[CrossRef](#)] [[PubMed](#)]

28. Pfeifer, S.; Crowder, C.; Harrington, L.; Brown, M. Secondary osteon and Haversian canal dimensions as behavioral indicators. *Am. J. Phys. Anthropol.* **2006**, *131*, 460–468. [[CrossRef](#)]
29. Mayya, A.; Banerjee, A.; Rajesh, R. Mammalian cortical bone in tension is non-Haversian. *Sci. Rep.* **2013**, *3*, 2533. [[CrossRef](#)]
30. Zedda, M.; Lepore, G.; Biggio, G.P.; Gadau, S.; Mura, E.; Farina, V. Morphology, morphometry and spatial distribution of secondary osteons in equine femur. *Anat. Histol. Embryol.* **2015**, *44*, 328–332. [[CrossRef](#)]
31. Frongia, G.N.; Muzzeddu, M.; Mereu, P.; Leoni, G.; Berlinguer, F.; Zedda, M.; Farina, V.; Satta, V.; Di Stefano, M.; Naitana, S. Structural features of cross-sectional wing bones in the griffon vulture (*Gyps fulvus*) as a prediction of flight style. *J. Morphol.* **2018**, *279*, 1753–1763. [[CrossRef](#)]
32. Frongia, G.N.; Naitana, S.; Farina, V.; Gadau, S.D.; Di Stefano, M.; Muzzeddu, M.; Leoni, G.; Zedda, M. Correlation between wing bone microstructure and different flight styles: The case of the griffon vulture (*Gyps fulvus*) and greater flamingo (*Phoenicopterus roseus*). *J. Anat.* **2021**, *239*, 59–69. [[CrossRef](#)] [[PubMed](#)]
33. Kolb, C.; Scheyer, T.M.; Lister, A.M.; Azorit, C.; de Vos, J.; Schlingemann, M.A.J.; Rössner, G.E.; Monaghan, N.T.; Sanchez-Villagra, M.R. Growth in fossil and extant deer and implications for body size and life history evolution. *BMC Evol. Biol.* **2015**, *15*, 19. [[CrossRef](#)] [[PubMed](#)]
34. Zedda, M.; Sathe, V.; Chakraborty, P.; Palombo, M.R.; Farina, V. A first comparison of bone histomorphometry in extant domestic horses (*Equus caballus* Linnaeus, 1758) and a Pleistocene Indian wild horse (*Equus namadicus* Falconer & Cautley, 1849). *Integr. Zool.* **2020**, *15*, 448–460. [[CrossRef](#)]
35. Palombo, M.R.; Zedda, M. The intriguing giant deer from the Bate cave (Crete): Could paleohistological evidence question its taxonomy and nomenclature? *Integr. Zool.* **2022**, *17*, 54–77. [[CrossRef](#)] [[PubMed](#)]
36. Parfitt, A.M.; Drezner, M.K.; Glorieux, F.H.; Kanis, J.A.; Malluche, H.; Meunier, P.; Ott, S.M.; Recker, R.R. Bone histomorphometry: Standardization of nomenclature, symbols, and units: Report of the ASBMR Histomorphometry Nomenclature Committee. *J. Bone Min. Res.* **1987**, *2*, 595–610. [[CrossRef](#)]
37. Zedda, M.; Babosová, R. Does the osteon morphology depend on the body mass? A scaling study on macroscopic and histomorphometric differences between cow (*Bos taurus*) and sheep (*Ovis aries*). *Zoomorphology* **2021**, *140*, 169–181. [[CrossRef](#)]
38. Lakes, R. On the torsional properties of single osteons. *J. Biomech.* **1995**, *28*, 1409–1410. [[CrossRef](#)]
39. Miszkiewicz, J. Investigating histomorphometric relationships at the human femoral midshaft in a biomechanical context. *J. Bone Min. Metab.* **2016**, *34*, 179–192. [[CrossRef](#)]
40. Wu, X.; Li, C.; Chen, K.; Sun, Y.; Yu, W.; Zhang, M.; Whang, Y.; Qin, Y.; Chen, W. Multi-scale mechanotransduction of the poroelastic signals from osteon to osteocyte in bone tissue. *Acta Mech. Sin.* **2020**, *36*, 964–980. [[CrossRef](#)]
41. Kepler, J. *Strena Seu de Nive Sexangula (The Six-Cornered Snowflake)*, 1st ed.; Gottfried Tampach: Frankfurt, Germany, 1611.
42. Hales, T.C. Historical overview of the Kepler conjecture. *Discret. Comput. Geom.* **2006**, *36*, 5–20. [[CrossRef](#)]
43. Hales, T.C.; Ferguson, S.P. A formulation of the Kepler conjecture. *Discret. Comput. Geom.* **2006**, *36*, 21–69. [[CrossRef](#)]
44. Marchal, C. Study of Kepler’s conjecture: The problem of the closest packing. *Math. Z.* **2011**, *267*, 737–765. [[CrossRef](#)]

Disclaimer/Publisher’s Note: The statements, opinions and data contained in all publications are solely those of the individual author(s) and contributor(s) and not of MDPI and/or the editor(s). MDPI and/or the editor(s) disclaim responsibility for any injury to people or property resulting from any ideas, methods, instructions or products referred to in the content.